Equations of State on Demand: Application for Surrogate Fuel Development

International Journal of Thermophysics
Journal of Thermophysical Properties and Thermophysics and Its Applications

ISSN 0195-928X
Volume 32
Number 3

Int J Thermophys (2011)
32:596-613
DOI 10.1007/s10765-010-0909-3

Volume 32 • Number 3 • March 2011

International Journal of Thermophysics

Available online
www.springerlink.com

IJOT • 10765 • ISSN 0195-928X
32(3) 549–736 (2011)

Springer

Springer

Springer

Int J Thermophys (2011) 32:596–613
DOI 10.1007/s10765-010-0909-3

Equations of State on Demand: Application for Surrogate Fuel Development

**Marcia L. Huber · Thomas J. Bruno ·
Robert D. Chirico · Vladimir Diky ·
Andrei F. Kazakov · Eric W. Lemmon ·
Chris D. Muzny · Michael Frenkel**

Received: 8 December 2010 / Accepted: 27 December 2010 / Published online: 15 January 2011

Abstract The NIST ThermoData Engine (TDE) is a large electronic database containing experimental data with detailed descriptions of relevant metadata and uncertainties that incorporates expert-system software to automatically generate dynamically evaluated data and on-demand equations of state. In this study, we demonstrate how the concept of dynamic data evaluation within the NIST TDE can be used to generate equations of state (EOS) on demand, and give an example where the resulting EOS formulations for pure chemical compounds are used to develop a surrogate mixture model to represent the volatility behavior, as expressed by the distillation curve, of a synthetic paraffinic aviation fuel derived from biomass.

Keywords Distillation curve · Equation of state · Helmholtz free energy · Surrogate model · ThermoData Engine

1 Introduction

Thermophysical and thermochemical property data represent key foundations for development and improvement of all chemical process technologies. In addition, high-quality property data are frequently essential prerequisites in the search for new relationships between properties of chemical systems, and constitute the basis of the scientific discovery process.

M. L. Huber (✉) · T. J. Bruno · R. D. Chirico · V. Diky · A. F. Kazakov · E. W. Lemmon ·
C. D. Muzny · M. Frenkel
Thermophysical Properties Division, National Institute of Standards and Technology,
325 Broadway, Boulder, CO 80305, USA
e-mail: Marcia.huber@nist.gov

Previously, we defined various data types (experimental, predicted, derived, and critically evaluated) within thermophysical and thermochemical properties [1]. Based on these considerations, critical data evaluation can be defined as a process of generation of critically evaluated property data based on available experimental and predicted data as well as their uncertainties. Critical evaluation of thermodynamic and thermophysical property data can be performed based on one of three general methods: (1) single-property data analysis; (2) simultaneous analysis of multiple properties with enforced mutual consistency; or (3) through application of an equation of state (EOS) [2,3]. Implementation of the EOS approach (when an ideal gas expression for the ideal gas heat capacity is available) allows, in principle, evaluation of all thermodynamic properties of the system simultaneously. In general, an EOS for a pure fluid establishes a relationship between the thermodynamic variables of the system, temperature T, molar volume V, and pressure p. For a pure substance, the EOS can generally be expressed as

$$pV = RT + f(T, p) \tag{1}$$

where R is the gas constant.

In the case of an ideal gas, where interactions between molecules are absent, the function $f(T, p)$ is equal to zero. In practice, this term is rarely negligible and has been calculated with a wide variety of numerical approximations leading to the development of hundreds of empirical EOS formulations during the last century [4].

We note that the first empirical formulation of the EOS was suggested by van der Waals [5] to take into account molecular size and molecular interaction forces, resulting eventually in recognition of this landmark scientific achievement by the Nobel prize in physics [6] in 1910. The purpose of this article is to demonstrate how new technologies designed to implement the concept of dynamic data evaluation [7–9] can be used to generate EOS on demand, and then to deploy the resulting EOS formulations for pure chemical compounds to model thermodynamic properties of a complex mixture, for example, an aviation fuel. We will specifically use the EOS formulations to develop a surrogate model for a synthetic paraffinic kerosene fuel derived from biomass (BIO-SPK).

2 Equations of State on Demand

Highly precise equations of state often contain numerous parameters for characterizing $f(T, p)$. These equations can be deployed only if the compound of interest has been studied adequately to allow determination of the fitting parameters. Data of high quality and broad range are often required for a high-precision EOS. Some less precise EOS formulations containing only a few parameters can be deployed for a large variety of "data scenarios," including compounds for which data are sparse. Until recently, EOS technology has been deployed in only static data evaluations, where critical data evaluation must be initiated far in advance of need.

NIST ThermoData Engine (TDE) [2,10–13] software represents the first full-scale implementation of the dynamic data evaluation concept for thermodynamic and thermophysical properties. This concept requires large electronic databases capable of storing essentially all relevant experimental data known to date with detailed descriptions of metadata (information necessary to interpret numerical data such as properties, variables, constraints, phases, etc.) and uncertainties. The combination of these electronic databases with expert-system software, designed to automatically generate recommended data based on available experimental and predicted data, leads to the ability to produce critically evaluated data dynamically or "to order."

EOS deployment in dynamic data evaluation is particularly challenging for complex, high-precision equations, due to mathematical complexities, the sensitivity of results to data quality, the necessity to meet special validation criteria, and the need to function without human intervention. Dynamic evaluation provides new opportunities for generating EOS representations for a wide variety of chemical species. A key aspect is the establishment of criteria for deployment of a specific type of EOS based on a particular data scenario, i.e., the data quality and extent. In order to adequately represent a range of data scenarios, four different equations of state of varying complexity and precision are currently selected for implementation in TDE [2]: Peng–Robinson [14], PC-SAFT [15], Sanchez-Lacombe [16,17], and fundamental equations based on the Helmholtz energy [18–20]. In this article, this selection was limited to Peng–Robinson and the Helmholtz EOS. These two forms illustrate the development of equations of state for two different data situations. The first case occurs when there are no data or extremely limited experimental data, and the Peng–Robinson EOS is applicable. The second situation is where there are sufficient experimental data for a variety of properties over a wide range of conditions to enable the development of a wide ranging, high-precision EOS such as the Helmholtz form.

2.1 The Peng–Robinson EOS

Over the years, many authors have proposed modifications to the EOS developed by van der Waals [5] in 1873. One of the more widely used modifications is that proposed by Peng and Robinson [14] in 1976. It may be expressed as [4,21]

$$Z = V(V-b)^{-1} - \Theta V/\{(RT)(V^2 + \delta V + \varepsilon)\}^{-1} \tag{2}$$

where Z is the compressibility factor ($pV/(RT)$), and the quantity Θ is defined based on the following expressions:

$$\Theta = \mathrm{A}\psi \tag{3}$$

where

$$\psi = \left\{\left(-0.26992\omega^2 + 1.54226\omega + 0.37464\right)\left(1 - T_\mathrm{r}^{0.5}\right) + 1\right\}^2 \tag{4}$$

$$A = 0.45724\,(RT_\mathrm{c})^2/p_\mathrm{c} \tag{5}$$

and

$$T_\mathrm{r} = T/T_\mathrm{c} \tag{6}$$

where ω is the acentric factor, T_c is the critical temperature, and p_c is the critical pressure. Finally, the equation quantities b, δ, and ε are defined as follows:

$$b = 0.0778RT_\mathrm{c}/p_\mathrm{c} \tag{7}$$

$$\delta = 2b \tag{8}$$

$$\varepsilon = -b^2 \tag{9}$$

Note that the original van der Waals equation can be recovered by setting $\delta = \varepsilon = 0$, and $\psi = 1$.

Implementation of the Peng–Robinson EOS requires only three parameters—T_c, p_c, and ω—making it easy to use when data are limited. When experimental data are unavailable, the TDE program uses predictive methods [22–26] to obtain the critical temperature, critical pressure, and the vapor–pressure curve. The acentric factor is calculated from its definition using the Ambrose–Walton equation [27] for the vapor pressure.

2.2 Fundamental EOS Formulations Based on the Helmholtz Energy

Most modern, wide-range, high-precision equations of state for pure fluid properties are fundamental equations explicit in the Helmholtz energy as a function of density and temperature. The term "fundamental equation" refers to an EOS that represents all the thermodynamic properties. Equations of state explicit in the Helmholtz energy as the fundamental property with independent variables of density and temperature can be expressed as

$$a(\rho, T) = a^0(\rho, T) + a^\mathrm{r}(\rho, T) \tag{10}$$

where $a^0(\rho, T)$ is the ideal gas contribution to the Helmholtz energy and $a^\mathrm{r}(\rho, T)$ is the residual Helmholtz energy, which corresponds to the influence of intermolecular forces. An advantage of the Helmholtz energy form is that all single-phase thermodynamic properties can be calculated as derivatives of the Helmholtz energy. For example,

$$p = \rho^2 \left(\frac{\partial a}{\partial \rho}\right)_T . \tag{11}$$

In addition, although the Peng–Robinson and other cubic equations of state are generally expressed in terms of pressure as a function of volume and temperature, one can obtain an expression for the dimensionless residual Helmholtz energy α^r by integration,

$$\alpha^\mathrm{r} = (a - a^0)/RT = \int (Z - 1)\rho^{-1}\,\mathrm{d}\rho. \tag{12}$$

The Helmholtz energy of the ideal gas is given by the expression

$$a^0(\rho, T) = h_0^0 + \int_{T_0}^{T} c_p^0(T')\,\mathrm{d}T' - RT - T\left[s_0^0 + \int_{T_0}^{T} \frac{c_p^0}{T'}\,\mathrm{d}T' - R\ln\left(\frac{\rho T}{\rho_0 T_0}\right)\right], \tag{13}$$

where ρ_0 is the ideal-gas density at T_0 and p_0 ($\rho_0 = p_0/T_0R$). The values of T_0, p_0, h_0^0, and s_0^0 are arbitrary, and can be chosen based on a user's desired reference values of enthalpy and entropy. Equation 13 requires an expression for the ideal-gas heat capacity, c_p^0. The TDE [10] program provides the ability to generate formulations for the ideal-gas heat capacity by use of several different functional forms. One such form [18,28] is expressed in terms of "Planck-Einstein" functions:

$$c_p^0 = c_0T^{c_1} + c_2\frac{(c_3/T)^2\exp(c_3/T)}{[1-\exp(c_3/T)]^2} + c_4\frac{(c_5/T)^2\exp(c_5/T)}{[1-\exp(c_5/T)]^2} + c_6\frac{(c_7/T)^2\exp(c_7/T)}{[1-\exp(c_7/T)]^2} \tag{14}$$

In Eq. 14, the temperature T is in K and c_p^0 is in $\mathrm{J\cdot mol^{-1}\cdot K^{-1}}$. This form of equation can extrapolate reliably to high temperatures and is superior to common polynomial fits that often have unphysical behavior when extrapolated beyond the range over which they were fitted. As is often the case, when experimental data for c_p^0 are unavailable, the TDE program provides estimates for the ideal-gas heat capacity by use of the method of Joback and Reid [22] with group parameters evaluated as described by Frenkel et al. [11]

A common functional form for the dimensionless residual Helmholtz energy [18] is

$$a^{\mathrm{r}}(\delta, \tau) = \Sigma N_k\delta^{d_k}\tau^{t_k} + \Sigma N_k\delta^{d_k}\tau^{t_k}\exp\left(-\delta^{l_k}\right) \tag{15}$$

where δ is the reduced density ($\delta = \rho/\rho_{\mathrm{c}}$) and τ is the inverse reduced temperature ($\tau = T_{\mathrm{c}}/T$). Each summation typically contains 4 to 20 terms, where the index k indicates each individual term. The values of d_k, t_k, and l_k are constrained such that the t_k are generally expected to be greater than zero, and d_k and l_k are integers greater than zero.

The specific fundamental equations of state used in TDE [2] are based on the work of Span and Wagner [19,20]. Their study describes the development of two 12-term equations with fixed functional forms: one for nonpolar or slightly polar substances, and one for polar fluids. Data sets of high quality were used to develop the functional forms and assess the quality of the resulting data representations. Although these "technical equations" suffer from a slight loss in representation accuracy for some compounds with very extensive high-quality data, their shorter forms allow for computations that are as much as ten times faster, depending on the number of terms in the other equations and on the use of special constraints for fitting in the critical region. The use of a fixed form also provides a well-behaved thermodynamic surface and helps to avoid overfitting of data.

3 Application to the Development of Surrogate Fuel Models

There has been a great deal of recent interest in fuels for gas turbine engines. This has included efforts to expand the scope of fuel feedstocks to include non-petroleum sources such as coal, natural gas, and biomass. As a consequence of this interest, there is a desire to develop thermophysical property models to correlate these properties, to enhance design and operational specifications for further application of new fuels.

A typical turbine fuel is a complex mixture of hundreds of components, and modeling each individual constituent and its interactions in the mixture is not feasible. Instead, we have been successful in the use of a surrogate mixture concept

Table 1 Potential constituent fluids for the surrogate fuel mixture

Compound	CAS no.	EOS	T_c (K)	T_b (K)	p_c (kPa)	ω
4-Methyloctane	2216-34-4	PR	574.8[a]	415.2[b]	2374[a]	0.5329
2,6-Dimethyloctane	2051-30-1	PR	603.7[c]	431.4[b]	2212[h]	0.4392
3-Methylnonane	5911-04-6	PR	614.2[a]	440.8[b]	2177[a]	0.4558
2,5-Dimethylnonane	17302-27-1	PR	619.0[d]	449.1[g]	1974[d]	0.4672
2-Methyldecane	6975-98-0	H	624.1[a]	462.3[b]	1885[f]	0.5626
n-Undecane	1120-21-4	H	638.8[b]	469.0[b]	2093[f]	0.5447
3,6-Dimethyldecane	17312-53-7	PR	640.0[d]	469.6[g]	1815[d]	0.4887
5-Ethyldecane	17302-36-2	PR	654.0[e]	480.4[f]	1790[e]	0.4891
3-Methylundecane	1002-43-3	PR	652.6[c]	485.5[b]	1696[h]	0.5425
n-Dodecane [53]	112-40-3	H	658.1[b]	489.44[b]	1817[f]	0.574
2,3,5-Trimethyldecane	62238-11-3	PR	663.7[e]	484.7[g]	1722[d]	0.4348
5-Methyldodecane	17453-93-9	PR	664.5[c]	501.0[b]	1832[h]	0.6457
n-Tridecane	629-50-5	H	675.6[b]	508.6[b]	1691[f]	0.6156
3-Methyltridecane	6418-41-3	PR	687.2[i]	522.8[b]	1553[h]	0.6472
2,5-Dimethyldodecane	56292-65-0	PR	669.0[d]	505.9[g]	1532[e]	0.5867
n-Tetradecane	629-59-4	H	692.5[b]	526.7[b]	1614[f]	0.6585
n-Pentadecane	629-62-9	H	706.9[b]	543.8[b]	1481[f]	0.6944

[a] Estimated by QSPR [26]
[b] Based on available experimental values
[c] Estimated by Joback method [22]
[d] Estimated by Marrero–Padillo method [54]
[e] Estimated by Constantinou–Gani method [23]
[f] Derived from EOS
[g] Estimated by NRRC [24] method
[h] Extrapolated from vapor pressure curve
[i] Estimated by Wilson–Jasperson method [25]

Table 2 Available experimental data for pure fluids (numbers refer to references)

Compound	Critical point	p_{sat}	ρ	c_p	Sound speed	ΔH_{vap}
4-Methyloctane		[55–57][a]	[58]			
2,6-Dimethyloctane		[59–63]	[63]			
3-Methylnonane		[64][a]	[65]			
2,5-Dimethylnonane		[66]	[67]			
2-Methyldecane		[68]	[69–72]	[73]		[74]
n-Undecane[b]	[75,76]	[77]	[78–80]	[81–83]	[84–87]	
3,6-Dimethyldecane						
5-Ethyldecane		[88,89][a]	[88,89]			
3-Methylundecane		[70]	[70]			
n-Dodecane	[53]	[53]	[53]	[53]	[53]	[53]
2,3,5-Trimethyldecane						
5-Methyldodecane		[70][a]	[70]			
n-Tridecane[b]	[90–96]	[72,77]	[78,80,97,98]	[82,97,99,100]	[97,101,102]	[76]
3-Methyltridecane		[70][a]	[70]			
2,5-Dimethyldodecane			[67]			
n-Tetradecane[b]	[1,90–92,94–96,103]	[77,104–107]	[80,108,109]	[82,110,111]	[86,101,102,111,112]	[76]
n-Pentadecane[b]	[90–92,94–96,113]	[72,77]	[114]	[82,115]	[86]	[75,76]

[a] Data only available at normal boiling point

[b] Only data sets covering wide ranges of T, p with low uncertainties are shown here. Other references with limited data are not shown for this fluid

Table 3 Equation-of-state parameters for *n*-undecane

Critical par.	T_c (K)	p_c (kPa)	ρ_c ($\mathrm{mol \cdot dm^{-3}}$)	
	638.815	2093	1.46256	
c_p^0 coeff. (Eq. 14)	c_0	c_1	c_2	c_3
	76.612	0.162002	127.359	1158.74
	c_4	c_5	c_6	c_7
	94.1326	3803.9	264.576	1830.25
EOS coeff. (Eq. 15)				
k	N_k	t_k	d_k	l_k
1	1.14538	0.25	1	0
2	−3.05196	1.125	1	0
3	0.879796	1.5	1	0
4	−0.281238	1.375	2	0
5	0.143417	0.25	3	0
6	0.000217543	0.875	7	0
7	1.04732	0.625	2	1
8	−0.0211113	1.75	5	1
9	−0.566096	3.625	1	2
10	−0.190717	3.625	4	2
11	−0.0335304	14.5	3	3
12	0.0129656	12	4	3

Validity range: 247.6 K to 721.9 K, 0 MPa to 655 MPa, $0\ \mathrm{kg \cdot m^{-3}}$ to $657.3\ \mathrm{kg \cdot m^{-3}}$
Molar mass: $156.308\ \mathrm{g \cdot mol^{-1}}$

[29–33] that incorporates advanced distillation curve (ADC) measurements [34–45] along with thermophysical property data measurements such as density, heat capacity, sound speed, viscosity, and thermal conductivity [46–49]. The general principle is to use a mixture with a relatively small number of components (usually <15) to represent the behavior of the actual complex fuel. Edwards and Maurice [50] provide an overview of the general requirements and expectations of fuel surrogates.

Surrogate fuel mixtures vary in complexity, and most are intended for specific purposes. In this study, the goal is to demonstrate the use of EOS on-demand technology to develop a surrogate model for a biomass-based fuel. We will limit the scope to providing a surrogate model that describes the volatility behavior, as shown by the advanced distillation curve [34–45]. The advanced distillation curve methodology [34–45] contains several important improvements in the measurement of distillation curves of complex fluids. The modifications to the classical measurement provide for (1) a composition-explicit data channel for each distillate fraction (for both qualitative and quantitative analyses); (2) temperature measurements that are true thermodynamic state points that can be modeled with an EOS; (3) temperature, volume, and pressure measurements of low uncertainty suitable for EOS development; (4) consistency with a century of historical data; (5) an assessment of the energy content of each distillate fraction; (6) trace chemical analysis of each distillate fraction; and (7) a corrosivity assessment of each distillate fraction. The composition-explicit channel is achieved with a new sampling approach that allows precise qualitative as well as quantitative

Table 4 Equation-of-state parameters for 2-methyldecane

Critical par.	T_c (K)	p_c (kPa)	ρ_c (mol $\cdot$ dm^{-3})	
	624.1	1885	1.47301	
c_p^0 coeff. (Eq. 14)	c_0	c_1	c_2	c_3
	93.3136	0.0932937	178.915	980.231
	c_4	c_5	c_6	c_7
	116.989	4223.07	288.374	1937.68
EOS coeff. (Eq. 15)				
k	N_k	t_k	d_k	l_k
1	1.18484	0.25	1	0
2	−3.07899	1.125	1	0
3	0.85337	1.5	1	0
4	−0.26841	1.375	2	0
5	0.139517	0.25	3	0
6	0.000223968	0.875	7	0
7	0.94863	0.625	2	1
8	−0.0205464	1.75	5	1
9	−0.598613	3.625	1	2
10	−0.19087	3.625	4	2
11	−0.0298327	14.5	3	3
12	0.0152613	12	4	3

Validity range: 224.3 K to 639.1 K, 0 MPa to 2.4 MPa, 0 kg $\cdot$ m^{-3} to 780.5 kg $\cdot$ m^{-3}
Molar mass: 156.308 g $\cdot$ mol^{-1}

analyses of each fraction, on the fly. It has been applied to the measurement of rocket propellant, gasolines, diesel fuels, jet fuels, and hydrocarbon crude oils. The most relevant feature applicable to this study is that the ADC provides temperature measurements that are true thermodynamic state points that can be modeled with an EOS.

The procedure for developing the surrogate mixture can be summarized as follows. First, a chemical analysis is performed to identify the major species present in the fuel sample. From this analysis, a list of representative fluids is constructed, including compounds chosen from the various chemical families (branched or linear paraffins, alkenes, aromatics, mono or polycyclic paraffins, etc.) found in the sample. The goal is try to develop a model that is chemically authentic—meaning that although the exact fluids that constitute the surrogate may not be present in the actual fuel, they do in fact represent the chemical types present in the real fuel. For each of these possible pure-fluid constituents, individual correlations for thermophysical properties are required. In this example, our goal is to match the volatility of the fuel, so we need only to develop an EOS. If, in addition, one also wants to model the thermal conductivity, viscosity, surface tension, or cetane number of a fuel, then models for these properties of the individual constituents are required as well. A mixture model is used that incorporates the pure-fluid equations for the thermodynamic properties. The fluids in the surrogate mixture and their compositions are then chosen by determining the surrogate composition that minimizes the difference between the predicted and the

Table 5 Equation-of-state parameters for *n*-tridecane

Critical par.	T_c (K)	p_c (kPa)	ρ_c (mol · dm^{-3})	
	675.634	1691	1.21625	
c_p^0 coeff. (Eq. 14)	c_0	c_1	c_2	c_3
	50.4642	0.278912	338.579	1534.11
	c_4	c_5	c_6	c_7
	103.942	2780.82	0.0	0.0
EOS coeff. (Eq. 15)				
k	N_k	t_k	d_k	l_k
1	1.39164	0.32	1	0
2	−2.87332	1.23	1	0
3	0.305134	1.5	1	0
4	−0.179527	1.4	2	0
5	0.093016	0.07	3	0
6	0.0002761	0.8	7	0
7	0.986319	2.16	2	1
8	0.0360788	1.1	5	1
9	−0.489974	4.1	1	2
10	−0.135264	5.6	4	2
11	−0.0302586	14.5	3	3
12	0.0147871	12	4	3

Validity range: 267.8 K to 690.6 K, 0 MPa to 500 MPa, 0 kg · m^{-3} to 897.7 kg · m^{-3}
Molar mass: 184.361 g · mol^{-1}

experimental data for the targeted properties, in this case, the points on the advanced distillation curve.

The fuel sample investigated here [51] is a biomass-to-liquid fuel (BIO-SPK). This fluid was converted to an isoparaffinic kerosene from a feedstock of animal fats, used cooking greases, and recovered brown greases. From the analysis by gas chromatography/mass spectrometry of the fuel sample [51], we compiled a list of potential candidate fluids for the surrogate model. These fluids are listed in Table 1. For each mono-branched alkane identified in the chemical analysis, a representative chemical species was selected as a candidate constituent fluid for the surrogates. Thus, for our purposes, all x-methylnonanes are represented as a single methylnonane. Similarly, we used a particular x, y-dimethylnonane to represent the dimethylnonane family. A major factor governing the specific choice of compound to represent a moiety was the availability of property data: priority was given to the selection of compounds for which the most abundant and reliable experimental measurements were available. For each possible constituent fluid, we searched the TDE [10] for experimental physical property data. For some of the fluids, the data were sparse and were supplemented with predicted values from the TDE. The available experimental data for each fluid are summarized in Table 2. Ideal-gas heat capacities based on group contribution methods were obtained from Frenkel et al. [52]. It is clear that many of the fluids are lacking in data and require the application of predictive methods. The predictive methods

Table 6 Equation-of-state parameters for *n*-tetradecane

Critical par.	T_c (K)	p_c (kPa)	ρ_c (mol · dm^{-3})	
	692.547	1614	1.14917	
c_p^0 coeff. (Eq. 14)	c_0	c_1	c_2	c_3
	30.175	0.348173	61.844	284.606
	c_4	c_5	c_6	c_7
	419.85	1696.05	0.0	0.0
EOS coeff. (Eq. 15)				
k	N_k	t_k	d_k	l_k
1	1.52213	0.32	1	0
2	−3.02849	1.23	1	0
3	0.294593	1.5	1	0
4	−0.183821	1.4	2	0
5	0.100939	0.07	3	0
6	0.000308913	0.8	7	0
7	1.00568	2.16	2	1
8	0.036571	1.1	5	1
9	−0.469823	4.1	1	2
10	−0.112874	5.6	4	2
11	−0.0293384	14.5	3	3
12	0.0128658	12	4	3

Validity range: 279.0 K to 707.5 K, 0 MPa to 150 MPa, 0 kg · m^{-3} to 796.1 kg · m^{-3}
Molar mass: 198.388 g · mol^{-1}

used and the values of the critical point and normal boiling point are summarized in Table 1.

Because our modeling approach [30,32] requires thermophysical property models for all pure constituent fluids, it was necessary to have available equations of state (for thermodynamic information) for each of the potential constituent pure fluids. Two different data scenarios are evident in this table. For six fluids (2-methyldecane, *n*-undecane, *n*-dodecane, *n*-tridecane, *n*-tetradecane, and *n*-pentadecane), there are sufficient data to develop a Helmholtz form EOS. (For these fluids, we have shown only some of the most wide ranging data sets and there may be additional data sets that contain only a single point or limited ranges of T and p that were not included in Table 2.) With the exception of *n*-dodecane, we used the TDE program to obtain the EOS coefficients for these fluids, and present them in Tables 3, 4, 5, 6, and 7. (For *n*-dodecane we used a previously developed Helmholtz EOS [53].) Figure 1a–d illustrates the percentage deviations between the Helmholtz EOS and several property types (vapor pressure, liquid density, heat capacity, and sound speed) for *n*-tridecane. Uncertainties of the experimental data are indicated by vertical lines. The quality of thermodynamic surface developed depends on the uncertainties of the underlying data used to develop the surface, but Fig. 1a–d illustrates typical performance for a Helmholtz EOS generated by the TDE program. Typically, one can expect liquid density to be represented to within 2 kg · m^{-3} to 5 kg · m^{-3}, liquid heat capacity up to the

Table 7 Equation-of-state parameters for *n*-pentadecane

Critical par.	T_c (K)	p_c (kPa)	ρ_c (mol · dm^{-3})	
	706.882	1481	1.06672	
c_p^0 coeff. (Eq. 14)	c_0	c_1	c_2	c_3
	43.3493	0.31566	26.192	197.899
	c_4	c_5	c_6	c_7
	386.293	1552.27	97.851	2654.94
EOS coeff. (Eq. 15)				
k	N_k	t_k	d_k	l_k
1	1.58458	0.32	1	0
2	−3.08023	1.23	1	0
3	0.302558	1.5	1	0
4	−0.186372	1.4	2	0
5	0.0971768	0.07	3	0
6	0.000300649	0.8	7	0
7	0.961799	2.16	2	1
8	0.0400807	1.1	5	1
9	−0.4855	4.1	1	2
10	−0.122765	5.6	4	2
11	−0.0346945	14.5	3	3
12	0.0199921	12	4	3

Validity range: 283.1 K to 721.9 K, 0 MPa to 654.6 MPa, 0 kg · m^{-3} to 893.2 kg · m^{-3}
Molar mass: 212.415 g · mol^{-1}

normal boiling point to within 5 J · mol^{-1} · K^{-1} to 10 J · mol^{-1} · K^{-1}, and sound speed to within 10 m · s^{-1} to 25 m · s^{-1}. As the critical region is approached, the deviations in heat capacity increase, since the heat capacity is infinite at the critical point. The representation of the vapor pressure is expected to be within 1 % to 2 % for pressures greater than about 1 kPa, with larger deviations at lower pressures.

For the remaining fluids, the data are extremely limited. For these fluids, we use the original Peng–Robinson EOS, which may be used when one has only T_c, p_c,and ω. In this study, we have used the original Peng–Robinson formulation to illustrate our procedure, but we note that for fluids with acentric factors greater than 0.49, Robinson and Peng [116] recommend an alternative formulation for Eq. 4. The values of the parameters are presented in Table 1. The vapor pressure curve can be predicted with the Ambrose–Walton method [27] and the acentric factor is obtained from its definition. We note that if one is interested in improving the representation of the liquid density, TDE has the ability to use the volume-translated modification [117] of the Peng–Robinson EOS. Since our objective is to model the volatility behavior, we have retained the original Peng–Robinson form for simplicity. This equation can represent the vapor pressure at pressures greater than 1 kPa to about 5 %, as illustrated in Fig. 2 for 3-methylundecane.

For calculations of the thermodynamic properties of mixtures, we used the mixture model [118–120] incorporated into the REFPROP database [121]. This model includes an algorithm for estimating binary interaction parameters when data are unavailable

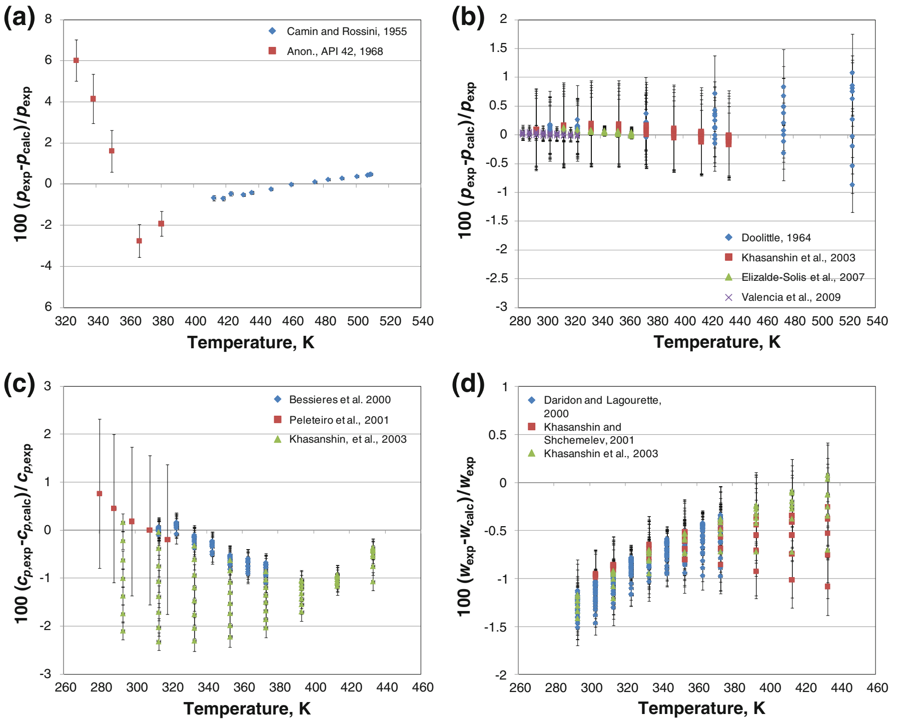

Fig. 1 (a) Deviations of experimental vapor-pressure data [72,77] from the Helmholtz EOS for *n*-tridecane, (b) deviations of experimental liquid-density data [78,80,97,98] from the Helmholtz EOS for *n*-tridecane, (c) deviations of experimental liquid heat-capacity data [97,99,100] from the Helmholtz EOS for *n*-tridecane, and (d) deviations of experimental liquid sound-speed data [97,101,102] from the Helmholtz EOS for *n*-tridecane

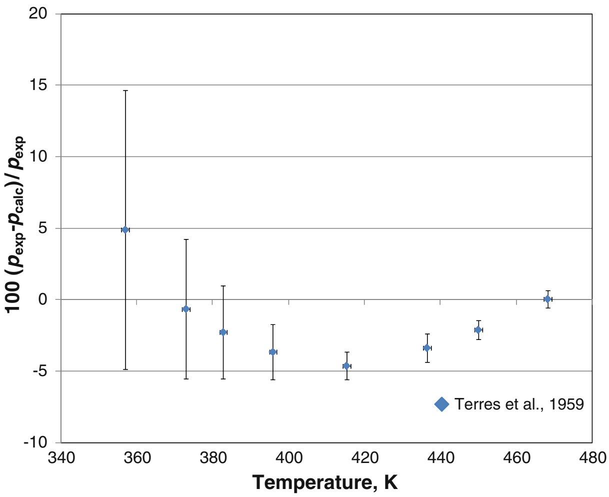

Fig. 2 Deviations of experimental vapor-pressure data [70] from the PR EOS for 3-methylundecane

Table 8 Compositions of the surrogate mixtures

Component	Composition, mole fraction		
	5-Component surrogate	4-Component surrogate	3-Component surrogate
4-Methyloctane	0.105	0.072	0
2,5-Dimethylnonane	0.281	0.409	0
2,3,5-Trimethyldecane	0.164	0	0
3-Methylnonane	0	0	0.458
n-Tridecane	0.227	0.317	0.356
n-Pentadecane	0.223	0.202	0.186

for a particular fluid pair. The estimation method is described in Lemmon and McLinden [119] and incorporates the critical temperature, critical pressure, acentric factor, and dipole moment for each pure fluid in the mixture. In addition, we used an algorithm developed in earlier study [32] to compute the distillation curve. The calculated points on the distillation curve can be compared directly with data from the advanced distillation curve metrology [34–40,44]. A nonlinear regression procedure was used to minimize the differences between the experimental distillation curve data [51] and the predictions of the model to determine the components and their relative abundances to define the surrogate fluid mixtures for the BIO-SPK fuel sample. The objective function was the sum of the squared percentage differences between the experimental data and the predicted values. The regression variables are the mole fraction compositions of the surrogate mixture components. Our initial slate included all the components in Table 1. Successive iterations gave very small concentrations of some components. These were removed from the mixture, and the minimization process was repeated until further reductions in the number of components resulted in unacceptably large deviations from the experimental data. The minimization algorithm proceeds until a minimum is located, and due to the complex nature of the search space, this may not be the absolute minimum. Runs from different starting points were tried to investigate alternative solutions.

The final compositions of the surrogate mixtures are summarized in Table 8. Three potential surrogates are shown. Figure 3 displays the distillation curves for 3-, 4-, and 5-component surrogate mixtures. The 5-component surrogate provides a good match of the distillation curve, to within 0.1 % (about 0.5 K). The experimental data are estimated to have an uncertainty on the order of 0.1 K to 0.3 K [51]. The 3- and 4-component surrogates demonstrate how the ability to model the distillation curve decreases as the number of constituent fluids decreases. In this study (consistent with the chemical analysis [51]), all the potential components are either branched or linear alkanes, and it is possible to model the mixture with a small number of constituent fluids. In a more complicated mixture, one generally needs more components, so that major chemical families are represented. The simple 5-component surrogate presented here captures the volatility behavior of the actual fuel sample to within 0.1 %, and demonstrates the use of the on-demand EOS technology for surrogate model development.

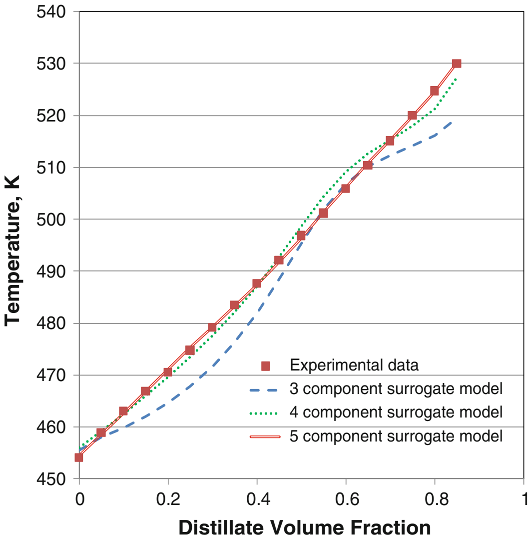

Fig. 3 Comparison of distillation curve data with several surrogate models

4 Conclusions

The TDE has been successfully deployed to generate on-demand equations of state for 17 possible constituent fluids used in the development of a surrogate model for a synthetic turbine fuel derived from biomass (BIO-SPK). Reliable full thermodynamic surfaces for each proposed component have been produced by the TDE depending on the availability of experimental data by use of either the Helmholtz energy (for six components) or Peng–Robinson equations of state. These equations were then used to develop a five-component surrogate model for a biomass-based aviation turbine fuel. The surrogate model has been demonstrated to represent the volatility of the fuel, as evidenced by the advanced distillation curve, to within 0.1 %.

Acknowledgments We acknowledge Dr. J. Tim Edwards of the Propulsion Directorate of the Air Force Research Laboratory, Wright Patterson Air Force Base, for the fuel sample used in this study. We also thank our NIST colleague, Dr. Mark McLinden, for helpful comments.

References

1. R.D. Chirico, M. Frenkel, V.V. Diky, K.N. Marsh, R.C. Wilhoit, J. Chem. Eng. Data **48**, 1344 (2003)
2. V. Diky, C.D. Muzny, E.W. Lemmon, R.D. Chirico, M. Frenkel, J. Chem. Inf. Model. **47**, 1713 (2007)
3. M. Frenkel, J. Chem. Eng. Data **54**, 2411 (2009). doi:10.1021/je800877f
4. B.E. Poling, J.M. Prausnitz, J.P. O'Connell, *The Properties of Gases and Liquids*, 5th edn. (McGraw-Hill, New York, 2001)
5. J.D. Van der Waals, *Over de Continuïteit van den Gas—en Vloeistoftoestand (On the Continuity of the Gas and Liquid State)* (Leiden University, Leiden, 1873)
6. J.D. Van der Waals, The Equation of State for Gases and Liquids. Nobel Lecture, December 12, 1910
7. R.C. Wilhoit, K.N. Marsh, Int. J. Thermophys. **20**, 247 (1999)
8. M. Frenkel, *Dynamic Compilation: A Key Concept for Future Thermophysical Data Evaluation in Forum 2000: Fluid Properties for New Technologies—Connecting Virtual Design with Physical*

Reality; NIST Special Publication 975, ed. by J.C. Rainwater, D.G. Friend, H.J.M. Hanley, A.H. Harvey, C.D. Holcomb, A. Laesecke, J.W. Magee, C. Muzny (Gaithersburg, MD, 2001)

9. M. Frenkel, Pure Appl. Chem. **77**, 1349 (2005)
10. M. Frenkel, R.D. Chirico, V. Diky, C. Muzny, A.F. Kazakov, *NIST ThermoData Engine, NIST Standard Reference Database 103b-Pure Compounds, Binary Mixtures, and Chemical Reactions, Version 4.0.* (National Institute of Standards and Technology, Standard Reference Data Program, Gaithersburg, MD, 2009)
11. M. Frenkel, R.D. Chirico, V. Diky, X.J. Yan, Q. Dong, C. Muzny, J. Chem. Inf. Model. **45**, 816 (2005)
12. V. Diky, R.D. Chirico, A.F. Kazakov, C.D. Muzny, M. Frenkel, J. Chem. Inf. Model. **49**, 503 (2009). doi:10.1021/ci800345c
13. M. Frenkel, R.D. Chirico, V.V. Diky, C. Muzny, A.F. Kazakov, J. Chem. Inf. Model. **49**, 2883 (2009)
14. D. Peng, D.B. Robinson, Ind. Eng. Chem. Fundam. **15**, 59 (1976)
15. J. Gross, G. Sadowski, Ind. Eng. Chem. Res. **40**, 1244 (2001)
16. N. Koak, R.A. Heidemann, Ind. Eng. Chem. Res. **35**, 4301 (1996)
17. R.A. Krenz, *Correlating the Fluid Phase Behavior of Polydisperse Polyethylene Solutions using the Modified Sanchez-Lacombe Equation of State* (University of Calgary, Alberta, 2005)
18. E.W. Lemmon, R.T. Jacobsen, J. Phys. Chem. Ref. Data **34**, 69 (2005)
19. R. Span, W. Wagner, Int. J. Thermophys. **24**, 1 (2003)
20. R. Span, W. Wagner, Int. J. Thermophys. **24**, 41 (2003)
21. R.C. Reid, J.M. Prausnitz, B.E. Poling, *The Properties of Gases and Liquids*, 4th edn. (McGraw-Hill, New York, 1987)
22. K.G. Joback, R.C. Reid, Chem. Eng. Commun. **57**, 233 (1987)
23. L. Constantinou, R. Gani, AIChE J. **40**, 1697 (1994)
24. Y. Nannoolal, J. Rarey, D. Ramjugernath, W. Cordes, Fluid Phase Equilib. **226**, 45 (2004). doi:10.1016/j.fluid.2004.09.001
25. G.M. Wilson, L.V. Jasperson, Presented at AIChE Meeting (New Orleans, LA, 1996)
26. A.F. Kazakov, C.D. Muzny, V.V. Diky, R.D. Chirico, M. Frenkel, Fluid Phase Equilib. **298**, 131 (2010)
27. D. Ambrose, J. Walton, Pure Appl. Chem. **61**, 1395 (1989)
28. W. Wagner, A. Pruss, J. Phys. Chem. Ref. Data **31**, 387 (2002)
29. M.L. Huber, E.W. Lemmon, A. Kazakov, L.S. Ott, T.J. Bruno, Energy Fuels **23**, 3790 (2009)
30. M.L. Huber, E.W. Lemmon, V. Diky, B.L. Smith, T.J. Bruno, Energy Fuels **22**, 3249 (2008)
31. M.L. Huber, E.W. Lemmon, L.S. Ott, T.J. Bruno, Energy Fuels **23**, 3083 (2009)
32. M.L. Huber, B.L. Smith, L.S. Ott, T.J. Bruno, Energy Fuels **22**, 1104 (2008)
33. M.L. Huber, E.W. Lemmon, T.J. Bruno, Energy Fuels **24**, 3565 (2010)
34. T.J. Bruno, Ind. Eng. Chem. Res. **45**, 4371 (2006)
35. T.J. Bruno, B.L. Smith, Ind. Eng. Chem. Res. **45**, 4381 (2006)
36. T.J. Bruno, Sep. Sci. Technol. **41**, 309 (2006)
37. B.L. Smith, T.J. Bruno, Int. J. Thermophys. **27**, 1419 (2006)
38. B.L. Smith, T.J. Bruno, Ind. Eng. Chem. Res. **46**, 297 (2007)
39. B.L. Smith, T.J. Bruno, Ind. Eng. Chem. Res. **46**, 310 (2007)
40. B.L. Smith, T.J. Bruno, Energy Fuels **21**, 2853 (2007)
41. T.J. Bruno, A. Laesecke, S.L. Outcalt, H.D. Seelig, B.L. Smith, *The properties of a 50/50 mixture of Jet-A and S-8, NISTIR 6647* (2007)
42. B.L. Smith, T.J. Bruno, J. Propul. Power **24**, 618 (2008)
43. T.M. Lovestead, T.J. Bruno, Energy Fuels **23**, 3637 (2009)
44. T.J. Bruno, B.L. Smith, Energy Fuels **20**, 2109 (2006)
45. L.S. Ott, T.J. Bruno, Energy Fuels **21**, 2778 (2007). doi:10.1021/ef070195x
46. S. Outcalt, A. Laesecke, K. Brumback, J. Propul. Power **25**, 1626 (2009)
47. S.L. Outcalt, A. Laesecke, M.B. Freund, Energy Fuels **23**, 1626 (2009)
48. T.J. Bruno, The Properties of S-8 and JP-10. (Report prepared for Wright Laboratory Aero Propulsion Power Directorate under MIPR F4FBEY6346G001, 2007)
49. T.J. Bruno, M.L. Huber, A. Laesecke, E.W. Lemmon, L.S. Ott, S. Outcalt, R. Perkins, H.-D. Seelig, B.L. Smith, *The Properties of S-8, NISTIR 6648* (National Institute of Standards and Technology, Boulder, 2007)
50. T. Edwards, L.Q. Maurice, J. Propul. Power **17**, 461 (2001)
51. T.J. Bruno, E. Baibourine, T.M. Lovestead, Energy Fuels **24**, 3049 (2010)

52. M. Frenkel, G.J. Kabo, K.N. Marsh, G.N. Roganov, *Thermodynamics of Organic Compounds in the Gas State*. TRC Data Series, vol. I. (1994)
53. E.W. Lemmon, M.L. Huber, Energy Fuels **18**, 960 (2004)
54. J. Marrero-Morejon, E. Pardillo-Fontdevila, AIChE J. **45**, 615 (1999)
55. R.T. Leslie, J.D. White, J. Res. NBS **15**, 211 (1935)
56. F.D. Rossini, Refin. Nat. Gasoline Manuf. **14**, 255 (1935)
57. F.D. Rossini, Oil Gas J. **33**, 61 (1935)
58. P.A. Bazhulin, S.A. Ukholin, T.F. Bulanova, A.V. Koperina, A.F. Plate, B.A. Kazanskii, Izv. Akad. Nauk SSSR, Ser. Khim. **481** (1949)
59. J. Timmermans, Bull. Soc. Chim. Belg. **30**, 62 (1921)
60. B.A. Arbuzov, Zh. Obshch. Khim. **3**, 28 (1933)
61. J. Pliva, F. Sorm, Collect. Czech. Chem. Commun. **14**, 274 (1949)
62. F. Sorm, A. Mleziva, Z. Arnold, Collect. Czech. Chem. Commun. **14**, 693 (1949)
63. Y.-R. Naves, D. Lamparsky, P. Ochsner, Bull. Soc. Chim. Fr. **3**, 645 (1961)
64. F.D. Rossini, Pet. Manag. **14**, 41 (1943)
65. J.M. Geist, M.R. Cannon, Ind. Eng. Chem. Anal. Ed. **18**, 611 (1946)
66. P.A. Levene, R.E. Marker, J. Biol. Chem. **95**, 1 (1932)
67. H. Pichler, A. Herlan, F. Obenaus, Brennst.-Chem. **43**, 199 (1962)
68. A.G. Osborn, D.R. Douslin, J. Chem. Eng. Data **19**, 114 (1974)
69. C.E. Boord, K.W. Greenlee, J.M. Derfer, *The Synthesis, Purification, and Properties of Hydrocarbons of Low Molecular Weight*. (American Petroleum Institute Research Project 45, Twelfth Annual Report, Ohio State University, June, 1950)
70. E. Terres, L. Brinkmann, D. Fischer, D. Huellstrung, W. Lorz, G. Weisbrod, Brennst. Chem. **40**, 279 (1959)
71. G. Mann, M. Muhlstad, J. Braband, E. Doring, Tetrahedron **23**, 3393 (1967)
72. Anonymous, *Properties of Hydrocarbons of High Molecular Weight* (American Petroleum Institute Research Project 42, Pennsylvania State University, 1968)
73. J.F. Messerly, H.L. Finke, J. Chem. Thermodyn. **3**, 675 (1971)
74. V. Majer, V. Svoboda, J. Pechacek, S. Hala, J. Chem. Thermodyn. **16**, 567 (1984)
75. E. Morawetz, J. Chem. Thermodyn. **4**, 139 (1972)
76. S. Sunner, C. Svensson, J. Chem. Soc.-Faraday Trans. I **75**, 2359 (1979)
77. D.L. Camin, F.D. Rossini, J. Phys. Chem. **59**, 1173 (1955)
78. A.K. Doolittle, J. Chem. Eng. Data **9**, 275 (1964)
79. R. Landau, A. Wuerflinger, Ber. Bunsenges. Phys. Chem. **84**, 895 (1980)
80. J.L. Valencia, D. Gonzalez-Salgado, J. Troncoso, J. Peleteiro, E. Carballo, L. Romani, J. Chem. Eng. Data **54**, 904 (2009). doi:10.1021/je8006875
81. H.M. Huffman, G.S. Parks, M. Barmore, J. Am. Chem. Soc. **53**, 3876 (1931)
82. H.L. Finke, M.E. Gross, G. Waddington, H.M. Huffman, J. Am. Chem. Soc. **76**, 333 (1954)
83. J. Peleteiro, J. Troncoso, D. Gonzalez-Salgado, J.L. Valencia, M. Souto-Caride, L. Romani, J. Chem. Thermodyn. **37**, 935 (2005). doi:10.1016/j.jct.2004.12.010
84. O.Z. Golik, I.I. Ivanova, Zh. Fiz. Khim. **36**, 1768 (1962)
85. Y.A. Neruchev, V.V. Zotov, N.F. Otpushchennikov, Zh. Fiz. Khim. **43**, 2843 (1969)
86. F. Plantier, J.L. Daridon, B. Lagourette, C. Boned, High Temps.-High Press. **32**, 305 (2000)
87. D. Bessieres, F. Plantier, J. Therm. Anal. Calorim. **89**, 81 (2007). doi:10.1007/s10973-006-8452-y
88. J.D. Gibson, *Olefins of Types I and II from Butadiene and the Relation of Their Physical Constants to Structure* (Ohio State University, Columbus, 1938)
89. K. Ziegler, H. Grimm, R. Willer, Justus Liebigs Ann. Chem. **542**, 90 (1939)
90. E. Mogollon, W.B. Kay, A.S. Teja, Ind. Eng. Chem. Fundam. **21**, 173 (1982)
91. R.L. Smith, M. Anselme, A.S. Teja, in *Proceedings of World Congress III Chem. Eng.*, Tokyo, vol. II (1986), pp. 135–139
92. R.L. Smith, A.S. Teja, W.B. Kay, AIChE J. **33**, 232 (1987)
93. G. Christou, *Critical Properties of Binary Mixtures* (University of Melbourne, Melbourne, 1988)
94. D.J. Rosenthal, A.S. Teja, AIChE J. **35**, 1829 (1989)
95. A.S. Teja, M. Gude, D.J. Rosenthal, Fluid Phase Equilib. **52**, 193 (1989)
96. M.J. Anselme, M. Gude, A.S. Teja, Fluid Phase Equilib. **57**, 317 (1990)
97. T.S. Khasanshin, A.P. Shchamialiou, O.G. Poddubskij, High Temps. High Press. **35-6**, 227 (2003). doi:10.1068/htjr095

98. O. Elizalde-Solis, L.A. Galicia-Luna, L.E. Camacho-Camacho, Fluid Phase Equilib. **259**, 23 (2007). doi:10.1016/j.fluid.2007.04.023
99. D. Bessieres, H. Saint-Guirons, J.L. Daridon, J. Therm. Anal. Calorim. **62**, 621 (2000)
100. J. Peleteiro, D. Gonzalez-Salgado, C.A. Cerdeirina, J.L. Valencia, L. Romani, Fluid Phase Equilib. **191**, 83 (2001)
101. J.L. Daridon, B. Lagourette, High Temps.-High Press. **32**, 83 (2000)
102. T.S. Khasanshin, A.P. Shchemelev, High Temp. **39**, 60 (2001)
103. D. Ambrose, Trans. Farad. Soc. **59**, 1988 (1963)
104. P. Kneisl, J.W. Zondlo, J. Chem. Eng. Data **32**, 11 (1987)
105. D.L. Morgan, R. Kobayashi, Fluid Phase Equilib. **97**, 211 (1994)
106. M. Casserino, D.R. Blevins, R.N. Sanders, Thermochim. Acta **284**, 145 (1996)
107. I. Mokbel, A. Blondel-Telouk, D. Vellut, J. Jose, Fluid Phase Equilib. **149**, 287 (1998)
108. P. Gouel, Bull. Cent. Rech. Explor.-Prod. Elf-Aquitaine **2**, 211 (1978)
109. K. Holzapfel, G. Goetze, F. Kohler, Int. DATA Ser. Sel. Data Mix. A. **1**, 38 (1986)
110. M.S. Benson, P.S. Snyder, J. Winnick, J. Chem. Thermodyn. **3**, 891 (1971)
111. J.M. Pardo, C.A. Tovar, D. Gonzalez, E. Carballo, L. Romani, J. Chem. Eng. Data **46**, 212 (2001). doi:10.1021/je000197a
112. T. Takagi, H. Teranishi, Fluid Phase Equilib. **20**, 315 (1985)
113. A.S. Teja, R.L. Smith Jr., AIChE J. **33**, 1560 (1987)
114. W.G. Cutler, R.H. McMickle, W. Webb, R.W. Schiessler, J. Chem. Phys. **29**, 727 (1958)
115. D. Bessieres, H. Saint-Guirons, J.L. Daridon, Phys. Chem. Liq. **39**, 301 (2001)
116. D.B. Robinson, D.Y. Peng, The Characterization of the Heptanes and Heavier Fractions for the GPA Peng-Robinson Programs, Research Report 28, Gas Processors Association (GPA), Tulsa, OK (1978)
117. A. Peneloux, E. Rauzy, R. Freze, Fluid Phase Equilib. **8**, 7 (1982)
118. E.W. Lemmon, R.T. Jacobsen, J. Phys. Chem. Ref. Data **33**, 593 (2004)
119. E.W. Lemmon, M.O. McLinden, in *Proceedings of Thermophysical Properties and Transfer Processes of New Refrigerants Conference* (International Institute of Refrigeration, Commission B1, Paderborn Germany, 2001), pp. 23–30
120. O. Kunz, R. Klimeck, W. Wagner, M. Jaeschke, *The GERG-2004 Wide-Range Reference Equation of State for Natural Gases and Other Mixtures* (Fortschr.-Ber. VDI, VDI-Verlag, Dusseldorf, Germany, 2007)
121. E.W. Lemmon, M.L. Huber, M.O. McLinden, NIST Standard Reference Database 23, NIST Reference Fluid Thermodynamic and Transport Properties Database (REFPROP): Version 8.0 (Standard Reference Data, National Institute of Standards and Technology, Gaithersburg, MD, 2007)